Inorg. Chem. **2007**, *46*, 1237–1249

Tetrahydroxy-*p*-benzoquinone as a Source of Polydentate O-Donor Ligands. Synthesis, Crystal Structure, and Magnetic Properties of the $[Cu(bpy)(dhmal)]_2$ Dimer and the Two-Dimensional $[\{SiW_{12}O_{40}\}\{Cu_2(bpy)_2(H_2O)(ox)\}_2]\cdot 16H_2O$ Inorganic–Metalorganic Hybrid

Santiago Reinoso,[†] Pablo Vitoria, Leire San Felices, Ainara Montero, Luis Lezama,* and Juan M. Gutiérrez-Zorrilla*

Departamento de Química Inorgánica, Facultad de Ciencia y Tecnología, Universidad del País Vasco, P.O. Box 644, E-48080 Bilbao, Spain

Received September 4, 2006

The use of tetrahydroxy-*p*-benzoquinone as a slow source of dihydroxymalonato and oxalato ligands led to the isolation under open-air mild reaction conditions of five different compounds, two of them prepared for the first time: $[Cu(bpy)(dhmal)]_2$ (**1**) and $[\{SiW_{12}O_{40}\}\{Cu_2(bpy)_2(H_2O)(ox)\}_2]\cdot 16H_2O$ (**5**) (bpy, 2,2′-bipyridine; dhmal, dihydroxymalonate; ox, oxalate). A possible mechanism for the oxidation of the benzoquinone to give the croconate dianion, which undergoes further ring-opening oxidation to decompose into dihydroxymalonate and oxalate, is proposed. All compounds have been characterized by elemental analysis, thermogravimetry, infrared spectroscopy, and powder X-ray diffraction. Single-crystal X-ray diffraction, electron paramagnetic resonance, and magnetic susceptibility measurements have been performed for compounds **1** and **5**. A complete band assignment of the experimental FT-IR spectra is given through comparison with the ones calculated using density functional theory (DFT). The neutral dimer **1** constitutes the first structurally characterized example of a transition metal–dhmal complex, and it contains two copper atoms bridged by two dihydroxymalonato ligands acting in a μ^2-κ^3O,O′,O″:κ^1O coordination fashion, so that an *equatorial–axial* $Cu_2(\mu^2\text{-}O)_2$ rhomboid core is formed. On the other hand, the inorganic–metalorganic hybrid compound **5** shows a two-dimensional arrangement of Keggin polyanions linked by one of the Cu atoms of the oxalate cationic dimers to give layers parallel to the $(10\bar{1})$ plane, the remaining ox–Cu–bpy fragments acting as interlamellar separators. In both cases, magnetic and EPR results are discussed with respect to the crystal structure of the compounds and, for compound **1**, also with respect to DFT calculations of the exchange coupling constant.

Introduction

Polyoxometalates[1] (POMs) constitute a large family of metal−oxygen cluster compounds of surprising compositional variability, electronic versatility, and topological diversity. These features endow them with applications in a wide range of fields, such as catalysis,[2] material science,[3] medicine,[4] or photochemistry,[5] in such a way that there are already more commercial applications of polyoxometalates than any other class of cluster compounds.[6] The functionalization of POMs with rare-earth or transition-metal (TM) coordination complexes to give hybrid inorganic−metalorganic compounds constitutes an emerging area of interest in recent years.[7] The inclusion of the metal−organic complex moiety can be achieved either to provide charge compensation (ionic-type compounds), to modify the inorganic POM surface or framework with organic ligands (discrete decorated polyanions), or to link the clusters into infinite ordered arrays of variable dimensionality (extended materials). The motivation for this functionalization lies on the possibility of combining the different features of the components to lead to novel structural architectures; to a rational design of new catalytic systems; to tailored electronic, optic, and magnetic properties; or to unexpected and more selective applications

* To whom correspondence should be addressed. E-mail: luis.lezama@ehu.es (L.L.), juanma.zorrilla@ehu.es (J.M.G.-Z.). Fax: +34946013500.
[†] Current address: School of Engineering and Science, International University Bremen (Jacobs University Bremen as of Spring 2007), P.O. Box 750 561, 28725 Bremen, Germany.

10.1021/ic061671m CCC: $37.00
Published on Web 01/23/2007

that arise from synergistic effects and, therefore, that are not associated with simple materials.

To date, several of these hybrid compounds based on vanadium[8] and molybdenum[9] isopolyanions have been reported; in contrast, the number of structurally characterized examples incorporating Keggin heteropolyanions and their derivatives as the inorganic component is still comparatively lower. Most of them are hydrothermally synthesized and consist of ionic-type compounds[10] or discrete decorated polyanions,[11] so that only a few examples of extended hybrid materials can be found in the literature. They mainly show a one-dimensional nature, solids of higher dimensionalities being even rarer and, in most cases, based on highly reduced multicapped clusters.[12]

Currently, we are exploring the applicability of Keggin-POMs and TM-carboxylate cationic complexes in the preparation of new magnetically attractive hybrid compounds. Using a building-block self-assembly synthetic procedure under open-air mild reaction conditions, we have been able to prepare different hybrid compounds on the basis

(1) (a) Pope, M. T.; Müller, A. *Angew. Chem., Int. Ed. Engl.* **1991**, *30*, 34. (b) *Polyoxometalates: From Platonic Solids to Antiretroviral Activity*; Pope, M. T., Müller, A., Eds.; Kluwer: Dordrecht, The Netherlands, 1994. (c) Hill, C. L., Ed. *Chem. Rev.* **1998**, *98*, special thematic issue. (d) *Polyoxometalate Chemistry: From Topology via Self-Assembly to Applications*; Pope, M. T., Müller, A., Eds.; Kluwer: Dordrecht, The Netherlands, 2001. (e) *Polyoxometalate Chemistry for Nanocomposite Design*; Pope, M. T., Yamase, T., Eds.; Kluwer: Dordrecht, The Netherlands, 2002. (f) *Polyoxometalate Molecular Science*; Borrás-Almenar, J. J., Coronado, E., Müller, A., Pope, M. T., Eds.; Kluwer: Dordrecht, The Netherlands, 2003. (g) Pope, M. T. In *Comprehensive Coordination Chemistry II*; McCleverty, J. A., Meyer, T. J., Eds.; Elsevier: Oxford, U.K., 2004.

(2) (a) Moffat, J. B. *Chem. Eng. Commun.* **1989**, *83*, 9. (b) Belanger, R.; Moffat, J. B. *J. Catal.* **1995**, *152*, 171. (c) Mizuno, N.; Misono, M. *J. Mol. Catal.* **1994**, *86*, 319. (d) Corma, A. *Chem. Rev.* **1995**, *95*, 559. (e) Hill, C. L.; Prosser-Mccartha, M. *Coord. Chem. Rev.* **1995**, *143*, 407. (f) Kozhevnikov, I. V. *Catal. Rev.−Sci. Eng.* **1995**, *37*, 311. (g) Hill, C. L., Ed. *J. Mol. Catal.* **1996**, *114* (1−3), special thematic issue. (h) Neumann, R. *Progr. Inorg. Chem.* **1998**, *47*, 317. (i) Okuhara, T.; Mizuno, N.; Misono, M. *Adv. Catal.* **1996**, *41*, 113. (j) Kuznetsova, L. I.; Maksimov, G. M.; Likholobov, V. A. *Kinet. Catal.* **1999**, *40*, 622. (k) Misono, M. *Chem. Commun. (Cambridge)* **2001**, 1141. (l) Khenkin, A. M.; Weiner, L.; Wang, Y.; Neumann, R. *J. Am. Chem. Soc.* **2001**, *123*, 8531. (m) Kozhevnikov, I. V. Catalysis by Polyoxometalates. *Catalysts for Fine Chemicals*, Vol 2; Wiley: Chichester, U.K., 2002. (n) Okun, N. M.; Anderson, T. M.; Hardcastle, K. I.; Hill, C. L. *Inorg. Chem.* **2003**, *42*, 6610. (o) Kiricsi, I., Ed. *Appl. Catal., A* **2003**, *256* (1), special thematic issue. (p) Hill, C. L. *Angew. Chem., Int. Ed.* **2004**, *43*, 402. (q) Won, B. K.; Voitl, T.; Rodríguez-Rivera, G. J.; Dumesic, J. A. *Science* **2004**, *305*, 1280.

(3) (a) Coronado, E.; Gómez-García, C. J. *Comments Inorg. Chem.* **1995**, *17*, 255. (b) Ouahab, L. *Coord. Chem. Rev.* **1998**, *178−180*, 1501. (c) Coronado, E.; Galán-Mascarós, J. R.; Giménez-Saiz, C.; Gómez-García, C. J. *Adv. Mater. Opt. Electron.* **1998**, *8*, 61. (d) Clemente-Juan, J. M.; Coronado, E. *Coord. Chem. Rev.* **1999**, *193−195*, 361. (e) Kurth, D. G.; Lehmann, P.; Volmer, D.; Müller, A.; Schwahn, D. *J. Chem. Soc., Dalton Trans.* **2000**, *3989*. (f) Clemente-León, M.; Coronado, E.; Delhaes, P.; Gómez-García, C. J.; Mingolaud, C. *Adv. Mater.* **2001**, *13*, 574. (g) Forment-Aliaga, A.; Coronado, E.; Feliz, M.; Gaita-Ariño, A.; Llusar, R.; Romero, F. M. *Inorg. Chem.* **2003**, *43*, 8019. (h) Müller, A.; Das, S. K.; Talismanov, S.; Roy, S.; Beckmann, E.; Bögge, H.; Schmidtmann, M.; Merca, A.; Berkle, A.; Allouche, L.; Zhou, Y.; Zhang, L. *Angew. Chem., Int. Ed.* **2003**, *42*, 5039. (i) Casañ-Pastor, N.; Gómez-Romero, P. *Front. Biosci.* **2004**, *9*, 1759. (j) Bassil, B. S.; Nellutla, S.; Kortz, U.; Stowe, A. C.; van Tol, J.; Dalal, N. S.; Keita, B.; Nadjo, L. *Inorg. Chem.* **2005**, *44*, 2659. (k) Mialane, P.; Dolbecq, A.; Marrot, J.; Riviere, E.; Sécheresse, F. *Chem. Eur. J.* **2005**, *11*, 1771. (l) Mal, S. S.; Kortz, U. *Angew. Chem., Int. Ed.* **2005**, *44*, 3777. (m) Kortz, U.; Hussain, F.; Reicke, M. *Angew. Chem., Int. Ed.* **2005**, *44*, 3773.

(4) (a) Michelon, M.; Hervé, M.; Hervé, G. *Biochim. Biophys. Acta* **1987**, *916*, 402. (b) Yamase, T.; Fujita, M.; Fukushima, K. *Inorg. Chim. Acta* **1988**, *151*, 15. (c) Chottard, G.; Hill, C. L.; Weeks, M. S.; Schinazi, R. F. *J. Med. Chem.* **1990**, *33*, 2767. (d) Inouye, Y.; Tale, Y.; Tokutake, Y.; Yoshida, T.; Yamamoto, A.; Yamase, T.; Nakamura, S. *Chem. Pharm. Bull.* **1990**, *38*, 285. (e) Barnard, D. L.; Hill, C. L.; Gage, T.; Matheson, J. E.; Huffman, J. H.; Sidwell, R.; Otto, M. I.; Schinazi, R. F. *Antiviral Res.* **1997**, *34*, 27. (f) Fukuda, N.; Yamase, T.; Tajima, Y. *Biol. Pharm. Bull.* **1999**, *22*, 463. (g) Rhule, J. T.; Hill, C. L.; Zheng, Z.; Schinazi, R. F. *Topics Biol. Inorg. Chem.* **1999**, *2*, 117. (h) Botto, I. M.; Barrio, D. A.; Egusquiza, M. G.; Cabello, C. I.; Cortizo, A. M.; Etcheverry, S. B. *Metal Ions Biol. Med.* **2002**, *7*, 159. (i) Wang, X.; Liu, J.; Li, J.; Yang, Y.; Liu, J.; Li, B.; Pope, M. T. *J. Inorg. Biochem.* **2003**, *94*, 279. (j) Wang, X.; Liu, J.; Pope, M. T. *Dalton Trans.* **2003**, 957.

(5) (a) Hou, Y.; Hill, C. L. *New J. Chem.* **1992**, *16*, 909. (b) Yamase, T. *Mol. Eng.* **1993**, *3*, 241. (c) Papaconstantinou, E. *Trends Photochem. Photobiol.* **1994**, *3*, 139. (d) Gómez-Romero, P.; Casañ-Pastor, N. *J. Phys. Chem.* **1996**, *100*, 12448. (c) Athanasios, M.; Hiskia, A.; Androulaki, E.; Dimitikali, D.; Papaconstantinou, E. *Phys. Chem. Chem. Phys.* **1999**, *1*, 437. (e) Yamase, T.; Prokop, P. V. *Angew. Chem., Int. Ed.* **2002**, *41*, 466. (f) Ruether, T.; Hultgren, V. M.; Timko, B. P.; Bond, A. M.; Jackson, W. R.; Wedd, A. G. *J. Am. Chem. Soc.* **2003**, *125*, 10133. (g) Hill, C. L. In *Comprehensive Coordination Chemistry II*; McCleverty, J. A., Meyer, T. J., Eds.; Elsevier: Oxford, U.K., 2004.

(6) Proust, A. *Actual. Chim.* **2000**, 55.

(7) Hu, C.; Wang, Y.; Li, Y.; Wang, E. *Chem J. Internet* **2001**, *3*, http://web.chemistrymag.org/cji/2001/036022re.htm, and references therein.

(8) See for example: (a) Li, G.; Shi, Z.; Xu, Y.; Feng, S. *Inorg. Chem.* **2003**, *42*, 1170. (b) Finn, R. C.; Sims, J.; O'Connor, C. J.; Zubieta, J. *J. Chem. Soc., Dalton Trans.* **2002**, *159*. (c) Laduca, R. L., Jr.; Rarig, R. S., Jr.; Zubieta, J. *Inorg. Chem.* **2001**, *40*, 607. (d) Do, J.; Jacobson, A. J. *Inorg. Chem.* **2001**, *4*, 598. (e) Hagrman, P. J.; Zubieta, J. *Inorg. Chem.* **2001**, *40*, 2800.

(9) See for example: (a) Lu, C.-Z.; Wu, C.-D.; Zhuang, H.-H.; Huang, J.-S. *Chem. Mater.* **2002**, *14*, 2649. (b) Rarig, R. S., Jr.; Zubieta, J. *J. Solid State Chem.* **2002**, *167*, 370. (c) Yang, W.; Lu, C.; Zhuang, H. *J. Chem. Soc., Dalton Trans.* **2002**, 2879. (d) Wu, C.-D.; Lu, C.-Z.; Zhuang, H.-H.; Huang, J.-S. *Inorg. Chem.* **2002**, *41*, 5636. (e) Hagrman, P. J.; Zubieta, J. *Inorg. Chem.* **2000**, *39*, 5218.

(10) (a) Inman, C.; Knaust, J. M.; Keller, S. W. *Chem. Commun. (Cambridge)* **2002**, 156. (b) San Felices, L.; Vitoria, P.; Gutiérrez-Zorrilla, J. M.; Lezama, L.; Reinoso S. *Inorg. Chem.* **2006**, *45*, 7748.

(11) (a) Wassermann, K.; Lunk, H. J.; Palm, R.; Fuchs, J.; Steinfeldt, N.; Stösser, R.; Pope, M. T. *Inorg. Chem.* **1996**, *35*, 3273. (b) Wei, X.; Dickman, M. H.; Pope, M. T. *Inorg. Chem.* **1997**, *36*, 130. (c) Wei, X.; Dickman, M. H.; Pope, M. T. *J. Am. Chem. Soc.* **1998**, *120*, 10254. (d) Xu, Y.; Zhang, K.-L.; Zhang, Y.; You, X.-Z.; Xu, J.-Q. *Chem. Commun. (Cambridge)* **2000**, *153*. (e) Wang, Y.; Hu, C.; Peng, J.; Wang, E.; Xu, Y. *J. Mol. Struct.* **2001**, *598*, 161. (f) García, Fidalgo, E.; Neels, A.; Stoeckli-Evans, H.; Süss-Fink, G. *Polyhedron* **2002**, *21*, 1921. (g) Nandini, Devi, R.; Burkholder, E.; Zubieta, J. *Inorg. Chim. Acta* **2003**, *348*, 150. (h) Yuan, M.; Li, Y.; Wang, E.; Tian, C.; Wang, L.; Hu, C.; Hu, N.; Jia, H. *Inorg. Chem.* **2003**, *42*, 3670. (i) Luan, G.; Li, Y.; Wang, S.; Wang, E.; Han, Z.; Hu, C.; Hu, N.; Jia, H. *Dalton Trans.* **2003**, 233. (j) Liu, C.-M.; Zhang, D.-Q.; Zhu, D.-B. *Cryst. Growth Des.* **2003**, *3*, 363. (k) Mialane, P.; Dolbecq, A.; Riviere, E.; Marrot, J.; Sécheresse, F. *Eur. J. Inorg. Chem.* **2004**, 33. (l) Han, Z.-G.; Zhao, Y.-L.; Peng, J.; Ma, H.-Y.; Liu, Q.; Wang, E. *J. Mol. Struct.* **2005**, *738*, 1.

(12) (a) Cui, X.-B.; Yang, G.-Y. *Chem. Lett.* **2002**, *1238*. (b) Luan, G.; Li, Y.; Wang, E.; Han, Z.; Hu, C.; Hu, N.; Jia, H. *J. Solid State Chem.* **2002**, *165*, 1. (c) Dolbecq, A.; Mialane, P.; Lisnard, L.; Marrot, J.; Sécheresse, F. *Chem. Eur. J.* **2003**, *9*, 2914. (d) Duan, L.-M.; Pan, C.-L.; Xu, J.-Q.; Cui, X.; Xie, F.-T.; Wang, T.-G. *Eur. J. Inorg. Chem.* **2003**, *2578*. (e) Lisnard, L.; Dolbecq, A.; Mialane, P.; Marrot, J.; Sécheresse, F. *Inorg. Chim. Acta* **2004**, *357*, 845. (f) Niu, J.-Y.; Wei, M.-L.; Wang, J.-P.; Dang, D.-B. *Eur. J. Inorg. Chem.* **2004**, *160*. (g) Han, Z.; Zhao, Y.; Peng, J.; Ma, H.; Liu, Q.; Wang, E.; Hu, N.; Jia, H. *Eur. J. Inorg. Chem.* **2005**, *264*. (h) Zhen, P.-Q.; Ren, Y.-P.; Long, L.-S.; Huang, R.-B.; Zheng, L.-S. *Inorg. Chem.* **2005**, *44*, 1190. (i) Lisnard, L.; Dolbecq, A.; Mialane, P.; Marrot, J.; Codjovi, E.; Sécheresse, F. *Dalton Trans.* **2005**, *3913*. (j) Gu, X.; Peng, J.; Shi, Z.; Chen, Y.; Han, Z.; Wang, E.; Ma, J.; Hu, N. *Inorg. Chim. Acta* **2005**, *358*, 3701. (k) Soumahoro, T.; Burkholder, E.; Ouellette, W.; Zubieta, J. *Inorg. Chim. Acta* **2005**, *358*, 606. (l) Dolbecq, A.; Mellot-Draznieks, C.; Mialane, P.; Marrot, J.; Férey, G.; Sécheresse, F. *Eur. J. Inorg. Chem.* **2005**, *3009*. (m) An, H.-Y.; Wang, E.-B.; Xiao, D. R.; Li, Y.-G.; Su, Z.-M.; Xu, L. *Angew. Chem., Int. Ed.* **2006**, *45*, 904.

of the copper−monosubstituted $[SiW_{11}O_{39}Cu(H_2O)]^{6-}$ Keggin heteropolyanion as the inorganic building block: on one hand, ionic compounds[13] and discrete polyanions[14] in combination with C-shaped μ-diacetatobis(phenanthrolinecopper) complexes; and, on the other hand, one-dimensional compounds with planar μ-oxalatobis(bipyridinecopper) metal−organic blocks.[15] Following with this strategy, we are extending this study to other TM cationic dimers with aromatic dianions belonging to the $C_6O_4X_2^{2-}$ family as bridging ligands between metal centers (X = O, Cl, Br, I, CN). In the course of our investigations, we found that when tetrahydroxy-*p*-benzoquinone (H_2thq, X = OH) is reacted with Cu^{II} and 2,2′-bipyridine (bpy), instead of acting as a bridging ligand, it oxidizes to give the croconate dianion $C_5O_5^{2-}$ (crc), which undergoes further ring-opening oxidation to decompose into dihydroxymalonate $C_3(OH)_2O_4^{2-}$ (dhmal) and oxalate $C_2O_4^{2-}$ (ox) dianions.

Here we report the synthesis, chemical, and spectroscopic characterization, X-ray crystal structure, and magnetic properties of $[Cu(bpy)(dhmal)]_2$ (**1**), the first structurally characterized TM-complex containing the dihydroxymalonate dianion as ligand, and $[\{SiW_{12}O_{40}\}\{Cu_2(bpy)_2(H_2O)(ox)\}_2]\cdot 16H_2O$ (**5**), a two-dimensional inorganic−metalorganic hybrid compound based on $[SiW_{12}O_{40}]^{4-}$ α-Keggin polyanions and μ-oxalatobis(bipyridinecopper) cationic complexes. Although both compounds can be directly synthesized starting from the corresponding carboxylic acids, they could only be isolated as single crystals suitable for X-ray diffraction studies by using tetrahydroxy-*p*-benzoquinone as a slow source of dihydroxymalonato and oxalato ligands.

Experimental Section

Materials and Methods. The $K_4[\alpha\text{-}SiW_{12}O_{40}]\cdot 17H_2O$ and $K_8[\alpha\text{-}SiW_{11}O_{39}]\cdot 13H_2O$ POM precursors were synthesized according to the procedure described in the literature.[16] All other chemicals were obtained from commercial sources and used without further purification. Carbon, hydrogen, and nitrogen were determined by organic microanalysis on a LECO CHNS 932 analyzer. Copper was determined on a Perkin-Elmer 4110ZL atomic absorption analyzer. Infrared spectra (FT-IR) for solid samples were obtained as KBr pellets on a Mattson 1000 infrared spectrometer. Thermogravimetric analysis (TGA) and differential thermal analysis (DTA) were carried out on a TA Instruments SDT 2960 thermobalance under a 100 mL/min flow of synthetic air; the temperature was ramped from 20 to 800 °C at a rate of 5 °C/min. Magnetic susceptibility was measured on a Quantum Design MPMS-7 SQUID magnetometer (*T* range, 2−300 K; applied field, 0.1 T; diamagnetic corrections estimated from Pascal's constants). Electron paramagnetic resonance (EPR) powder spectra were recorded on a Bruker ESP300 spectrometer (X- and Q-bands) equipped with Oxford low-temperature devices (magnetic field calibration, NMR probe; determination of the frequency inside the cavity, Hewlett-Packard 5352B microwave frequency counter; maintenance of the crystal structures in the powder samples was confirmed by powder X-ray diffraction; computer simulation, WINEPR-Simfonia, version 1.5, Bruker Analytische Messtechnik GmbH).

Synthesis of $K_6[SiW_{11}O_{39}Cu(H_2O)]\cdot nH_2O$ Precursor. A solution of $K_8[SiW_{11}O_{39}]\cdot 13H_2O$ (6.44 g, 2 mmol) in a 1 M acetic acid/potassium acetate buffer (80 mL) was added to a solution of $Cu(NO_3)_2\cdot 3H_2O$ (0.5 g, 2.1 mmol) in water (20 mL). The reaction mixture was heated to 100 °C for 45 min and, after cooling to room temperature, an excess of solid KCl (19.5 g) was added. The $K_6[SiW_{11}O_{39}Cu(H_2O)]\cdot nH_2O$ precursor is obtained as a pale green powder after stirring for 18 h. Yield: 3.92 g (60% based on W). FT−IR (cm^{-1}). Main bands obsd (DFT-calcd): $\nu_{as}(Si-O_c) + \nu_{as}(W-O_t)$ (asymmetric coupling), 1011w (992); $\nu_{as}(W-O_t)$, 958s (915); $\nu_{as}(Si-O_c) + \nu_{as}(W-O_t)$, (symmetric coupling) 903vs (888); $\nu_{as}(W-O_e-W)$, 798vs and 742s (812 and 744); $\nu_{as}(Cu-O)$, 687 m (694); $\delta(W-O_e-W)$, 540w and 527w (535 and 517); $\delta(W-O_v-W)$, 491sh (481).

Synthesis of $[Cu(bpy)(dhmal)]_2$ (1), $[Cu(bpy)(H_2O)(crc)]$ (2), and $[\{Cu(bpy)(PF_6)\}_2(ox)]$ (3). (a) Method A (Single Crystal). A solution of tetrahydroxy-*p*-benzoquinone (34 mg, 0.2 mmol) in water (20 mL) was dropwise added to a solution of $CuCl_2\cdot 2H_2O$ (68 mg, 0.4 mmol) and 2,2′-bipyridine (62 mg, 0.4 mmol) in a water:methanol mixture (20:10 mL). The resulting dark-red solution was left to slowly evaporate at room temperature, and, after 2 days, greenish-brown crystals of compound **2** were removed by filtration. The resulting green mother liquors were left again to slowly evaporate, and compound **1** was obtained after 1 month as prismatic blue crystals suitable for single-crystal X-ray diffraction. If excess KPF_6 is added to the green mother liquors, a dark-blue crystalline powder of compound **3** is obtained after 2 weeks instead of complex **1**.

(b) Method B (Powder). A solution of disodium dihydroxymalonate (72 mg, 0.4 mmol) in water (20 mL) was added to a solution of $CuCl_2\cdot 2H_2O$ (68 mg, 0.4 mmol) and 2,2′-bipyridine (62 mg, 0.4 mmol) in a water:methanol mixture (40:20 mL). Compound **1** was obtained as a blue powder after stirring for 18 h. Yield: 92 mg (65% based on Cu).

(c) Compound 1. Anal. Calcd (found) for $C_{26}H_{20}Cu_2N_4O_{12}$: C, 44.14 (42.91); H, 2.85 (3.01); N, 7.92 (7.84). FT-IR (cm^{-1}). Main bands obsd (DFT-calcd): ν(O4−H), 3415s (3726m); ν(O5−H), 3202m (3564m); ν(C−H), 3116m, 3063m and 3040w (3264w, 3237w and 3211w); ν_{as}(O2−C−O3), 1663vs (1771vs); ν_{as}(O1−C−O6), 1642vs (1734s); $\nu_{as}(C-C)_{bpy} + \nu_{as}$(C−N), 1616s and 1574m (1655w and 1632w); $\nu(\text{bridge})_{bpy}$, 1499w (1532w); $\nu_{as}(C-C)_{bpy} + \nu_s$(C−N), 1478w (1515w); $\nu_s(C-C)_{bpy} + \nu_s$(C−N), 1448m (1492w); δ_{ip}(C−O5−H) + $\nu(C-C)_{dhmal}$, 1398s (1468w and 1379vs); $\nu(\text{ring})_{bpy}$, 1325w and 1253w (1355w and 1307w); δ_{ip}(C−O4−H), 1294m (1322m); ν(C−O5), 1182s (1192s); δ_{ip}(C−C−H), 1125w (1136w); $\delta_{ip}(C-C-C)_{dhmal} + \nu$(C−O4), 1049m (1055m); $\delta_{ip}(\text{ring})_{bpy}$, 1034m (1033w); wag(HO−C−OH), 978w (978w); δ_{ip}(O−C−O) + ν(Cu−O), 856w (844w); $\delta_{ip}(C-C-C)_{dhmal} + \delta_{oop}$(C−C−O), 822m (813w); δ_{oop}(C−C−O) + ν(Cu−O), 809w (789w); δ_{oop}(C−C−H), 783s (771m); $\delta_{oop}(\text{ring})_{bpy}$, 733w (740w); $\delta_{ip}(\text{ring})_{bpy} + \nu$(Cu−N), 662m (644w and 644w); δ(OH−C−OH), 563w (554w); δ_{oop}(C−O5−H), 544w (502w); δ_{ip}(OH−C−OH) + ν(Cu−O4), 460w (446w). TGA/DTA. The thermal analysis shows that compound **1** is anhydrous and stable up tp 135 °C, after which it undergoes three overlapped exothermic mass losses to lead to CuO as the final product at 295 °C [residue calcd (found): 22.5% (20.8)].

(d) Compound 2. Anal. Calcd (found) for $C_{15}H_{10}CuN_2O_6$: C, 47.69 (47.35); H, 2.67 (2.63); N, 7.41 (7.35). FT−IR (cm^{-1}): 1678 m, 1604s, 1509vs, 1448s, 781m. Single-crystal XRD. Triclinic

(13) Reinoso, S.; Vitoria, P.; San Felices, L.; Lezama, L.; Gutiérrez-Zorrilla, J. M. *Chem. Eur. J.* **2005**, *11*, 1538.
(14) Reinoso, S.; Vitoria, P.; San Felices, L.; Lezama, L.; Gutiérrez-Zorrilla, J. M. *Inorg. Chem.* **2006**, *45*, 108.
(15) (a) Reinoso, S.; Vitoria, P.; Lezama, L.; Luque, A.; Gutiérrez-Zorrilla, J. M. *Inorg. Chem.* **2003**, *42*, 3709. (b) Reinoso, S.; Vitoria, P.; Gutiérrez-Zorrilla, J. M.; Lezama, L.; San Felices, L.; Beitia, J. I. *Inorg. Chem.* **2005**, *44*, 9731.
(16) Tézé, A.; Hervé, G. *Inorg. Synth.* **1990**, *27*, 85.

crystal system, $P\bar{1}$ space group, $a = 7.163(3)$ Å, $b = 9.294(4)$ Å, $c = 11.901(4)$ Å, $\alpha = 69.20(3)°$, $\beta = 84.98(3)°$, $\gamma = 69.12(4)°$, $V = 691(1)$ Å^3.

(e) Compound 3. Anal. Calcd (found) for $C_{22}H_{16}Cu_2F_{12}N_4O_4P_2$: C, 32.33 (32.38); H, 1.97 (2.57); N, 6.85 (6.98). FT−IR (cm^{-1}): 1655vs, 1450s, 858vs, 816s, 773m, 731m, 556s, 477m. Powder XRD. Monoclinic crystal system, *C*2/*m* space group, $a = 14.493(2)$ Å, $b = 14.021(1)$ Å, $c = 7.944(1)$ Å, $\beta = 121.829(5)°$, $V = 1371.5(2)$ Å.^{3}

Synthesis of $K_2[\{SiW_{11}O_{39}Cu(H_2O)\}\{Cu_2(bpy)_2(H_2O)_2(ox)\}_2]\cdot 14H_2O$ (4) and $[\{SiW_{12}O_{40}\}\{Cu_2(bpy)_2(H_2O)(ox)\}_2]\cdot 16H_2O$ (5). (a) Method A (Single Crystal). A solution of $CuCl_2\cdot 2H_2O$ (68 mg, 0.4 mmol), 2,2′-bipyridine (62 mg, 0.4 mmol), and tetrahydroxy-*p*-benzoquinone (34 mg, 0.2 mmol) in a water:methanol mixture (40:10 mL) was dropwise added to a solution of $K_6[SiW_{11}O_{39}Cu(H_2O)]\cdot nH_2O$ (670 mg) in water (50 mL), and a brown precipitate was formed, which was removed by filtration. The resulting dark orange solution was left to slowly evaporate at room temperature, and a blue crystalline powder of compound **4** appeared after 1 week. This powder was also removed, and the resulting pale yellow mother liquors were left again to slowly evaporate. Compound **5** was obtained after 1 month as prismatic blue crystals suitable for single-crystal X-ray diffraction.

(b) Method B (Powder). Compound **5** was obtained as a blue powder by adding a solution of $CuCl_2\cdot 2H_2O$ (68 mg, 0.4 mmol), 2,2′-bipyridine (62 mg, 0.4 mmol) and oxalic acid (25 mg, 0.2 mmol) in a water:methanol mixture (30:10 mL) to a solution of $K_4[SiW_{12}O_{40}]\cdot 17H_2O$ (670 mg, 0.2 mmol) in water (50 mL). Yield: 740 mg (87% based on W).

(c) Compound 5. Anal. Calcd (found) for $C_{44}H_{36}Cu_4N_8O_{50}SiW_{12}\cdot 16H_2O$: C, 12.42 (12.51); H, 1.61 (1.39); N, 2.63 (2.62); Cu, 5.98 (5.89). FT-IR (cm^{-1}). Main bands obsd (DFT-calcd) for the $[Cu_2(bpy)_2(H_2O)(ox)]^{2+}$ block: δ(H−O−H) and υ_{as}(O−C−O)+υ_{as}(C−C)$_{bpy}$, 1653s and 1612sh (1662vs and 1619m); υ_{as}(C−C)$_{bpy}$+υ_{as}(C−N), 1570w (1599sh); υ(bridge)$_{bpy}$, 1498w (1504m); υ_{as}(C−C)$_{bpy}$+υ_s(C−N), 1471w (1485 m); υ_s(C−C)$_{bpy}$+υ_s(C−N), 1446m (1463m); υ_s(O−C−O), 1350w (1369m); υ(ring)$_{bpy}$, 1315w and 1252w (1333m and 1283s); δ_{ip}(C−C−H), 1159w and 1107w (1186w, 1174w and 1107m); δ_{ip}(ring)$_{bpy}$, 1059w and 1038w (1031m and 1018sh); δ_{oop}(C−C−H), 764s (772s); δ_{ip}(ring)$_{bpy}$+δ_{oop}(C−C−H), 727m (728w); δ_{ip}(ring)$_{bpy}$+υ(Cu−N), 667w and 648w (665w and 639w); δ_{ip}(C−C−O), 415w (415m); main bands obsd (DFT-calcd) for the $[SiW_{12}O_{40}]^{4-}$ block: ν_{as}(Si−O$_c$) + ν_{as}(W−O$_t$), (asymmetric coupling) 1012m (1005); ν_{as}(W−O$_t$), 968s (961); ν_{as}(Si−O$_c$) + ν_{as}(W−O$_t$), (symmetric coupling) 920vs (929); ν_{as}(W−O$_v$−W), 881m (899); ν_{as}(W−O$_e$−W), 796vs (828); δ(W−O$_e$−W), 534m (532); δ(W−O$_v$−W), 478w (505). TGA/DTA. The thermal decomposition of compound **5** takes place through four highly overlapped steps: it starts at room temperature with an endothermic dehydration process involving the release of at least 14 water molecules below 170 °C, after which it undergoes three exothermic mass losses to lead to the final residue at 510 °C. The thermogravimetric final residue is composed of monoclinic WO_3 (PDF No. 83-0951),[17] triclinic $CuWO_4$ (PDF No. 88-0269),[18] and most probably, amorphous SiO_2, as shown by powder X-ray diffraction [residue calcd (found) for $8WO_3 + 4CuWO_4 + 1SiO_2$: 75.1% (74.3)].

X-ray Data Collection and Structure Determination. Experimental details and crystal data for compounds **1** and **5** are given in Table 1. Data collection for the single-crystal X-ray diffraction (XRD) studies of **1** and **5** was performed at room temperature on an Xcalibur single-crystal diffractometer (Mo Kα radiation, $\lambda = 0.710\ 73$ Å) fitted with a Sapphire CCD detector. A total of 1120 (1148) frames of data was collected with exposure time of 70 s (25 s) per frame, using the ω-scan technique with frame width of $\Delta\omega = 0.50°$ (0.40°), for compound **1** (**5**). Data frames were processed (unit cell determination, intensity data integration, correction for Lorentz and polarization effects, and analytical absorption correction) using the CrysAlis software package.[19] Neutral atom scattering factors and anomalous dispersion factors were taken from the literature.[20] The structures were solved using direct methods (DIRDIF99)[21] and refined by full-matrix least-squares analysis with the SHELXL-97 program.[22] The positions of the aromatic H atoms were calculated geometrically and refined as riding atoms using default SHELXL parameters. The H atoms of the dihydroxymalonate ligand in compound **1** were located in a Fourier difference map. Thermal vibrations were treated anisotropically for all non-hydrogen atoms in compound **1** and only for W, Cu, and Si atoms in compound **5**. All calculations were performed using the WinGX crystallographic software package.[23]

Table 1. Crystallographic Data for Compounds **1** and **5**

	1	**5**
formula	$C_{26}H_{20}Cu_2N_4O_{12}$	$C_{44}H_{68}Cu_4N_8O_{66}SiW_{12}$
fw (g·mol^{-1})	707.6	4253.5
Cryst syst	triclinic	monoclinic
space group	$P\bar{1}$	$P2_1/n$
a (Å)	8.4965(6)	14.440(1)
b (Å)	9.3315(11)	13.423(1)
c (Å)	9.7891(10)	23.497(3)
α (deg)	60.807(11)	
β (deg)	68.977(8)	104.44(1)
γ (deg)	88.397(7)	
V (Å^3)	622.1(1)	4410.5(7)
Z	1	2
F(000)	358	3868
D_{calc} (g·cm^{-3})	1.889(1)	3.176(1)
μ (mm^{-1})	1.791	16.645
collctd reflcns	4170	28 094
unique reflcns (R_{int})	2401 (0.032)	8646 (0.077)
obsd reflcns [$I > 2\sigma(I)$]	1545	3829
refined params	204	323
goodness of fit (*S*)	0.875	0.977
$R(F_o)^a$ (obsd reflcns)	0.0393	0.0736
$R_w(F_o^2)^a$ (all reflcns)	0.0754	0.1323

^{a} $R(F_o) = \sum||F_o| - |F_c||/\sum|F_o|$; $R_w(F_o^2) = \{\sum[w(F_o^2 - F_c^2)^2]/\sum[w(F_o^2)^2]\}^{1/2}$.

Powder X-ray diffraction (XRD) studies of compounds **1**, **3,** and **5** were performed at room temperature on a Phillips PW-1470 X'Pert diffractometer (Cu Kα_1 radiation, $\lambda = 1.540\ 59$ Å) with Bragg−Brentano geometry. Data were collected by scanning in the 2θ range of 5−50° with increments of 0.02° and an exposure time of 10 s/increment. The powder XRD patterns of the thermogravimetric final residues of compounds **1** and **5** were registered at room

(17) Woodward, P. M.; Sleight, A. W.; Vogt, T. *J. Phys. Chem. Solids* **1995**, *56*, 1305.
(18) Schoefield, P. F.; Knight, K. S.; Redfern, S. A. T.; Cressey, G. *Acta Crystallogr.* **1997**, *B53*, 102.
(19) *CrysAlis CCD and RED*, version 1.70; Oxford Diffraction: Oxford, U.K., 2003.
(20) *International Tables for X-ray Crystallography*; Kynoch Press: Birmingham, U.K., 1974.
(21) Beurkens, P. T.; Beurkens, G.; de Gelder, R.; García-Granda, S.; Gould, R. O.; Israel, R.; Smits, J. M. M. *The DIRDIF Program System*; Crystallography Laboratory, University of Nijmegen: Nijmegen, The Netherlands, 1999.
(22) Sheldrick, G. M. *SHELXL97*; University of Göttingen: Göttingen, Germany, 1999.
(23) Farrugia, L. J. *J. Appl. Crystallogr.* **1999**, *32*, 837.

temperature on a Phillips PW-1700 diffractometer (Cu $K\alpha_1$ radiation, $\lambda = 1.540\,59$ Å) with Bragg−Brentano geometry. Data were collected by scanning in the 2θ range of 5−40° with increments of 0.02° and an exposure time of 5 s/increment. In all cases, the pattern matching was performed by using the FULLPROF program.[24]

Computational Details. All the quantum calculations have been carried out using the Gaussian03 program[25] running on computers with GNU/Linux operating systems. Density functional theory and specifically Becke's hybrid method with three parameters[26] based on nonlocal exchange and correlation funtionals, as implemented in Gaussian03 (B3LYP), has been used in all calculations. The optimization procedure for the $[SiW_{11}O_{39}Cu(H_2O)]^{6-}$ and $[SiW_{12}O_{40}]^{4-}$ polyanions[13] and the $[\{Cu(bpy)(H_2O)_2\}_2(\mu\text{-ox})]^{2+}$ cationic complex[15b] has been previously reported. Experimental data were used as the starting point in the global optimization of the binuclear $[\{Cu(bpy)(dhmal)\}_2]$ neutral complex (C_i, $S = 1$). The standard 6-31G(d)[27] basis has been chosen for all atoms. This basis contains polarization functions[28] in all atoms, except hydrogen. Infrared and Raman spectra were calculated on the optimized geometry of the four mentioned species. The infrared active vibrational frequencies were identified using the GaussviewW 3.0 program,[29] which provides a visual representation of the vibrational modes. In all cases, the DFT-calculated infrared spectra were in fair agreement with the experimental ones, so that a complete band assignment of the latter could be given by comparison with the formers.

The exchange coupling constant J_{ij} (defined through the phenomenological Heisenberg Hamiltonian: $H_{ij} = -J_{ij}S_iS_j$) of the binuclear $[\{Cu(bpy)(dhmal)\}_2]$ neutral complex has been calculated using the broken-symmetry computational strategy of Ruiz et al.,[30] which has been shown to provide good results as compared to experimental data. This calculation has used the experimental structure, since the calculated coupling constants are very sensitive to small deviations in the geometrical parameters. For the evaluation of the coupling constant of the copper(II) dimer complex, two separate DFT calculations have been carried out, from which the energies of the triplet state (E_{HS}) and a broken-symmetry singlet configuration (E_{BS}) are obtained, whereupon the coupling constant is approximately:

$$J_D = E_{BS} - E_{HS}$$

Several combinations of the recently developed double- to quadruple-ζ valence basis set of Weigend and Ahlrichs,[31] with polarization functions for all the atoms with the exception of hydrogens, was used in order to calculate the coupling constant.

Results and Discussion

Synthesis. In an attempt to synthesize a cationic Cu^{II}−bpy dimer with the thq dianion as bridging ligand, we reacted a water:methanol mixture (solution A, pH ∼ 3) of $CuCl_2$, bipyridine, and tetrahydroxy-*p*-benzoquinone in a 2:2:1 ratio. However, instead of acting as a bridging ligand, we observed that the benzoquinone was oxidized to give the croconate dianion, which underwent further ring-opening oxidation to decompose into dihydroxymalonate and oxalate dianions. Thus, no Cu^{II} complex containing the thq ligand was obtained from this experiment. As can be seen in Scheme 1, in a first stage greenish-brown crystals of the Cu^{II}−crc complex $[Cu(bpy)(H_2O)(crc)]$ (**2**) were isolated from the dark-red solution A after 2 days. The identification of this compound, which was previously reported by Castro et al.,[32] was acomplished by means of elemental analysis, FT-IR spectroscopy, and single-crystal XRD. If the Cu^{II}−crc complex is removed, in a second stage the Cu^{II}−dhmal neutral dimer **1** is obtained as blue single crystals from the resulting green mother liquors (solution B) after 1 month. The complete evaporation of solution B leads to a green precipitate, whose infrared spectrum shows characteristic bands of a Cu^{II}−bpy complex with a bridging ox ligand in a bis(bidentate) coordination fashion and whose elemental analysis is in good agreement with that calculated for the formula $[\{Cu(bpy)\}_2(ox)]Cl_2\cdot H_2O$.[33] This Cu^{II}−ox cationic dimer can be isolated by using bulky inorganic anions as crystallizing agents, such as hexafluorophosphate. Thus, when an excess of KPF_6 is added to solution B, a dark-blue crystalline powder of $[\{Cu(bpy)(PF_6)\}_2(ox)]$ (**3**) is obtained after 2 weeks instead of complex **1**. Compound **3**, which was previously reported by Thomas et al.,[34] was identified by means of elemental analysis, FT-IR spectroscopy, and powder XRD.

According to this observations, the tetrahydroxy-*p*-benzoquinone is a convenient slow source of oxalate dianions to in situ generate $[\{Cu(bpy)\}_2(ox)]^{2+}$ building blocks for the preparation under open-air mild reaction conditions of inorganic−metalorganic hybrid compounds containing bulky inorganic anions, such as Keggin-type POMs. In this way, the addition of solution A to an aqueous solution of the potassium salt of the Cu^{II}−monosubstituted $[SiW_{11}O_{39}Cu(H_2O)]^{6-}$ Keggin-type POM leads to an

(24) Rodríguez-Carvajal, J. *Physica* **1992**, *192*, 55.
(25) Frisch, M. J.; Trucks, G. W.; Schlegel, H. B.; Scuseria, G. E.; Robb, M. A.; Cheeseman, J. R.; Montgomery, J. A., Jr.; Vreven, T.; Kudin, K. N.; Burant, J. C.; Millam, J. M.; Iyengar, S. S.; Tomasi, J.; Barone, V.; Mennucci, B.; Cossi, M.; Scalmani, G.; Rega, N.; Petersson, G. A.; Nakatsuji, H.; Hada, M.; Ehara, M.; Toyota, K.; Fukuda, R.; Hasegawa, J.; Ishida, M.; Nakajima, T.; Honda, Y.; Kitao, O.; Nakai, H.; Klene, M.; Li, X.; Knox, J. E.; Hratchian, H. P.; Cross, J. B.; Bakken, V.; Adamo, C.; Jaramillo, J.; Gomperts, R.; Stratmann, R. E.; Yazyev, O.; Austin, A. J.; Cammi, R.; Pomelli, C.; Ochterski, J. W.; Ayala, P. Y.; Morokuma, K.; Voth, G. A.; Salvador, P.; Dannenberg, J. J.; Zakrzewski, V. G.; Dapprich, S.; Daniels, A. D.; Strain, M. C.; Farkas, O.; Malick, D. K.; Rabuck, A. D.; Raghavachari, K.; Foresman, J. B.; Ortiz, J. V.; Cui, Q.; Baboul, A. G.; Clifford, S.; Cioslowski, J.; Stefanov, B. B.; Liu, G.; Liashenko, A.; Piskorz, P.; Komaromi, I.; Martin, R. L.; Fox, D. J.; Keith, T.; Al-Laham, M. A.; Peng, C. Y.; Nanayakkara, A.; Challacombe, M.; Gill, P. M. W.; Johnson, B.; Chen, W.; Wong, M. W.; Gonzalez, C.; Pople, J. A. *Gaussian 03*, revision C.02; Gaussian, Inc.: Wallingford, CT, 2004.
(26) Becke, A. D. *J. Chem. Phys.* **1993**, *98*, 5648.
(27) (a) Wachters, A. J. H. *J. Chem. Phys.* **1970**, *52*, 1033. (b) Hay, P. J. *J. Chem. Phys.* **1977**, *66*, 4377. (c) Raghavachari, K.; Trucks, G. W. *J. Chem. Phys.* **1989**, *91*, 1062.
(28) Frisch, M. J.; Pople, J. A.; Winkley, J. S. *J. Chem. Phys.* **1984**, *80*, 3265.
(29) *GaussviewW*, version 3.0; Gaussian, Inc.: Wallingford, CT, 2004.
(30) Ruiz, E.; Alemany, P.; Álvarez, S.; Cano, J. *J. Am. Chem. Soc.* **1997**, *119*, 1297.
(31) Weigend, F.; Ahlrichs, R. *Phys. Chem. Chem. Phys.* **2005**, *7*, 3297.
(32) Castro, I.; Sletten, J.; Faus, J.; Julve, M. *J. Chem. Soc., Dalton Trans.* **1992**, 2271.
(33) Anal. Calcd (found) for $C_{22}H_{18}Cl_2Cu_2N_4O_5$: C, 42.87 (42.19); H, 2.94 (3.34); N, 9.09 (9.10). FT-IR (cm^{-1}): 1649vs, 1449m, 784s, 730m, 480m.
(34) Thomas, A. M.; Mandal, G. C.; Tiwary, S. K.; Rath, R. K.; Chakravarty, A. R. *J. Chem. Soc., Dalton Trans.* **2000**, 1395.

Scheme 1. Synthetical Routes for Compounds **1**−**5**

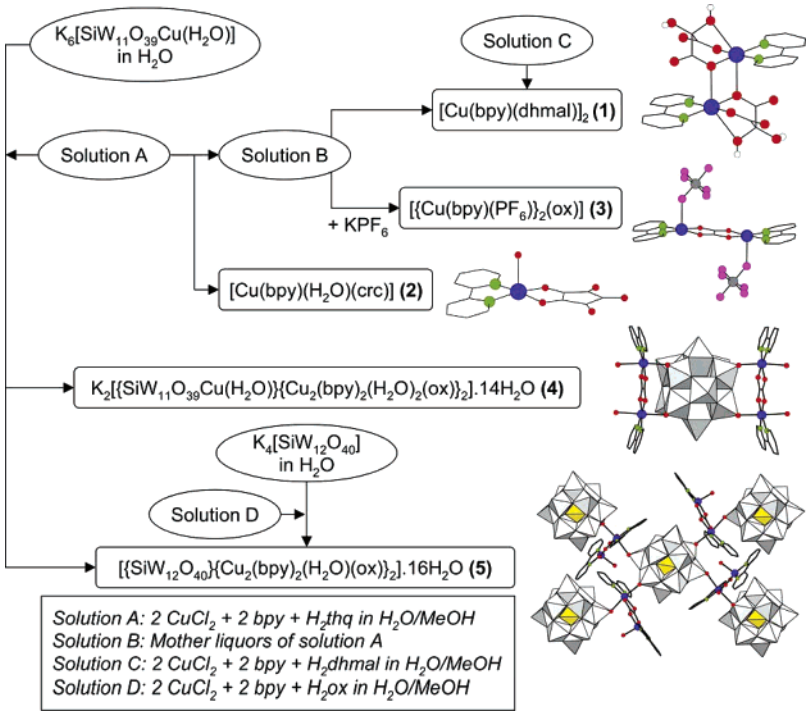

orange reaction mixture from which the discrete hybrid polyanion $[\{SiW_{11}O_{39}Cu(H_2O)\}\{Cu_2(bpy)_2(H_2O)_2(ox)\}_2]^{2-}$ (**4**), recently reported by our group,[15b] is isolated as a blue crystalline powder after 1 week. After removal of this compound, in 1 month the resulting pale yellow mother liquors yield the two-dimensional inorganic−metalorganic hybrid compound **5** as blue single crystals. The formation of this compound involves, besides the oxidation of tetrahydroxy-*p*-benzoquinone into oxalate, the transformation of the Cu^{II}-monosubstituted Keggin POM into its parent "complete" cluster $[SiW_{12}O_{40}]^{4-}$, which is not surprising if the acidity of the reaction medium (pH ∼ 3) and the pH stability range of the monolacunary keggin tungstosilicate anions (pH 4−6) is considered.[35]

As shown by powder XRD analysis[36] (see Supporting Information), both compounds **1** and **5** can be directly synthesized starting from the corresponding carboxylic acids: in the former case, from a water:methanol solution containing $CuCl_2$, bipyridine, and dihydroxymalonic acid disodium salt in a 1:1:1 ratio; and in the latter, by addition of a water:methanol solution containing $CuCl_2$, bipyridine, and oxalic acid in a 2:2:1 ratio to an aqueous solution of the $K_4[SiW_{12}O_{40}]$ POM precursor. However, in both cases they were isolated as precipitates which could not be recrystallized. Since other crystallization techniques did not give any successful result, the use of tetrahydroxy-*p*-benzoquinone as a slow source of dihydroxymalonato and oxalato ligands was the only method that allowed us to isolate compounds **1** and **5** as single crystals suitable for X-ray diffraction analysis.

Reaction Mechanism. A possible mechanism for the oxidation of H_2thq into croconate anion, followed by subsequent ring-opening oxidation of the latter into dihydroxymalonate and oxalate dianions, can be proposed on the basis of the literature (Scheme 2). The pK_a values of the benzoquinone (4.8 and 6.8)[37] indicate that it will behave in solution as a dianion with negative charges in an 1,4-arrangement. Thus, in the presence of 2 equiv of Cu^{II} and bipyridine it could act as a bridging ligand to form a cationic dimer analogous to those reported with related $C_6O_4X_2^{2-}$ ligands,[38] which would be expected to display an equilibrium with its corresponding monomeric neutral complex (Cu^{II}−thq), as in the case of the Cu^{II}−ox dimers.[39]

The Cu^{II} complexes with N-donor ligands are known to show catecholase activity and catalyze the oxidation of *o*-diphenols into *o*-quinones.[40] The proposed intermediate for this reaction consists of a Cu^{I} complex with a radicalary semiquinone anion originated from an intramolecular electronic transfer from the ligand to the metal. This type of intermediate has been detected by EPR spectroscopy, and it is in equilibrium with its parent Cu^{II} complex, the formation constant being very low. Taking into account that the thq ligand displays a catechol substructure, an analogous intramolecular electronic transfer for the Cu^{II}−thq monomer

(35) Tézé, A.; Hervé, G. *J. Inorg. Nucl. Chem.* **1977**, *39*, 2151.
(36) Powder XRD. Compound **1**: triclinic, $P\bar{1}$, $a = 8.486(2)$ Å, $b = 9.413(1)$ Å, $c = 9.886(1)$ Å, $\alpha = 60.24(1)°$, $\beta = 69.56(1)°$, $\gamma = 88.75(1)°$, $V = 631.2(3)$ Å^3. Compound **5**: monoclinic, $P2_1/n$, $a = 14.452(1)$ Å, $b = 13.431(1)$ Å, $c = 23.344(2)$ Å, $\beta = 104.76(1)°$, $V = 4352.0(7)$ Å^3.
(37) Preisler, P. W.; Berger, L.; Hill, E. S. *J. Am. Chem. Soc.* **1947**, *69*, 326.
(38) Fujii, C.; Mitsumi, M.; Kodera, M.; Motoda, K.; Ohba, M.; Matsumoto, N.; Okawa, H. *Polyhedron* **1994**, *13*, 933.
(39) (a) Castro, I.; Faus, J.; Julve, M.; Gleizes, A. *J. Chem. Soc., Dalton Trans.* **1991**, *1937*. (b) Castro, I.; Faus, J.; Julve, M.; Muñoz, M. C.; Díaz, W.; Solans, X. *Inorg. Chim. Acta* **1991**, *179*, 59. (c) Castro, I.; Faus, J.; Julve, M.; Mollar, M.; Monge, A.; Gutiérrez-Puebla, E. *Inorg. Chim. Acta* **1989**, *161*, 97.
(40) (a) Kaizer, J.; Pap, J.; Speier, G.; Parakanyi, L.; Korecz, L.; Rockenbauer, A. *J. Inorg. Biochem.* **2002**, *91*, 190. (b) Selmeczi, K.; Reglier, M.; Giorgi, M.; Speier, G. *Coord. Chem. Rev.* **2003**, *245*, 191.

Scheme 2. Proposed Mechanism for the Oxidation of Tetrahydroxy-*p*-benzoquinone into Croconate in the Presence of Cu^{II} and 2,2′-Bipyridine

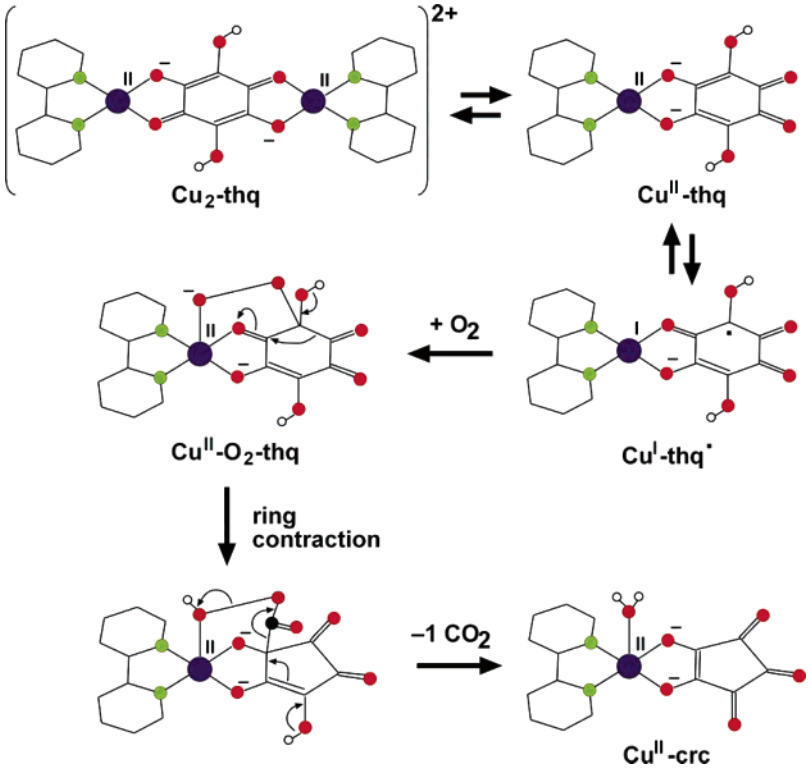

could be a priori expected, which would lead to the formation of a Cu^{I}−thq$^{\bullet}$ species. According to the model for the oxidation of the TM−semiquinone complexes,[41] this species can uptake an O_2 molecule, which would bind the metal center and the radicalary position to generate a Cu^{II}-peroxo-semiquinone intermediate (Cu^{II}−O_2−thq). The formation of the peroxo−carbon bond resembles the hydroxyl addition to rhodizonate dianion $C_6O_6^{2-}$, which promotes the formation of croconate dianion, CO_2, and water after ring contraction.[42] Thus, the Cu^{II}−O_2−thq intermediate could undergo a similar contraction process to give the corresponding five-membered ring substituted with a peroxocarboxilic group, which could be eliminated as CO_2 and water to lead to the croconate dianion and subsequent formation of compound **2**. This type of ring contraction of a peroxo-semiquinone intermediate has been previously proposed by Speier et al. to explain the isolation of [{Cu(tmen)}$_2$(μ-ox)(crc)] (tmen, tetramethylethylenediamine) from a mixture of Cu^0 and C_6O_6.[43]

According to the studies by Fabre et al.,[44] in an acidic aqueous medium (pH < 4) the croconate dianion is in equilibrium with its monohydrated form, which under aerobic conditions and the exposure to light has been shown to be unstable and to oxidize to give oxalic and dihydroxymalonic acids, the intermediate for this process being a cyclic diene over which 1,4-additions of O_2 molecules take place. Therefore, in this situation compound **2** would be expected to slowly evolve and to give Cu^{II}−dhmal and Cu^{II}−ox complexes, as the formation of the neutral dimer **1** and the isolation by a Keggin POM crystallizing agent of a Cu^{II}−ox cationic dimer in the hybrid compound **5** indicates.

Crystal Structure of Compound 1. To date, there is a reduced number of compounds related to the dihydroxymalonate dianion whose crystal structures have been reported in the literature, namely, the dihydroxymalonic acid,[45] the benzylethylammonium salt of dihydroxymalonate,[45] and the manganese(II)[46] and zinc(II)[47] complexes of the 2-hydroxy-2-hydroxylatemalonate trianion. Thus, to our knowledge compound **1** constitutes the first structurally characterized example of a TM complex containing the dihydroxymalonate dianion as ligand.

Figure 1 shows the ORTEP view of the centrosymmetric neutral dimer [Cu(bpy)(dhmal)]$_2$, together with the atom labeling scheme. Selected bond lengths and angles are given in Table 2. It is made of two dihydroxymalonate anions acting as μ^2-κ^3O,O′,O″:κ^1O bridges between two copper atoms which are separated by 3.49 Å. Each copper atom is involved in tetragonally elongated octahedral $CuN_2O_2O'_2$ chromophores with two bipyridine N atoms and two O atoms belonging to the carboxylate groups of one dihydroxymalonate ligand in the equatorial plane, the Cu−N and Cu−O bond lengths ranging from 1.93 to 1.99 Å. Due to this, the carboxylate C−O bonds are not symmetrical, those involving

(41) Barbaro, P.; Bianchini, C.; Linn, K.; Mealli, C.; Meli, A.; Vizza, F.; Laschi, F.; Zannello, P. *Inorg. Chim. Acta* **1992**, *198*−*200*, 31.
(42) West, R.; Niu, J. In *The Chemistry of the Carbonyl Group*; Zabicky, J., Ed.; Wiley: New York, 1970; p 241.
(43) Speier, G.; Speier, E.; Noll, B.; Pierpoint, C. G. *Inorg. Chem.* **1997**, *36*, 1520.
(44) Fabre, P. L.; Castan, P.; Deguenon, D.; Paillous, N. *Can. J. Chem.* **1995**, *73*, 1298.
(45) Aakeröy, C. B.; Nieuwenhuyzen, M.; Robinson, P. *J. Chem. Crystallogr.* **1998**, *28*, 111.
(46) Shi, J.-M.; Zhu, S.-C.; Liu, W.-D. *Transition Met. Chem.* **2004**, *29*, 358.
(47) Shi, J.-M.; Zhu, S.-C.; Wu, C.-J. *Jiegou Huaxue* **2004**, *23*, 1027.

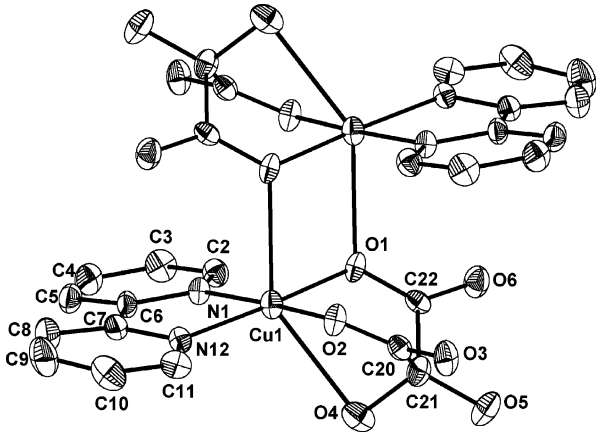

Figure 1. ORTEP view of the centrosymmetric neutral dimer [Cu(bpy)(dhmal)]$_2$ in compound **1**, together with the atom labeling scheme. Hydrogen atoms have been omitted for clarity.

Table 2. Selected Bond Lengths (Å) and Angles (deg) for Compound **1**[a]

	Cu1 Coordination Sphere		
Cu1−O1	1.967(2)	O1−Cu1−O2	91.8(1)
Cu1−O2	1.933(2)	O1−Cu1−O1^{i}	77.6(1)
Cu1−N1	1.987(3)	O1−Cu1−O4	71.6(1)
Cu1−N12	1.989(2)	O2−Cu1−O4	73.3(1)
Cu1−O1^{i}	2.494(3)	N1−Cu1−N12	81.3(1)
Cu1−O4	2.604(3)	N1−Cu1−O4	108.4(1)
		N12−Cu1−O4	110.8(1)
Cu1···Cu1^{i}	3.494(1)	Cu1−O1−Cu1^{i}	102.4(1)
	dhmal Ligand		
C22−O1	1.285(5)	O2−C20−O3	125.6(3)
C20−O2	1.272(5)	O1−C22−O6	124.7(4)
C20−O3	1.228(5)	O4−C21−O5	112.2(3)
C22−O6	1.229(4)	C20−C21−C22	108.6(3)
C21−O4	1.430(4)		
C21−O5	1.374(5)		
	Distortion Measures[b]		
Cu1−bpy1	9.0(1)	equatorial distortion	0.4(1)
Cu1−Cu$_2$O$_2$	89.5(1)	Cu1−Cu$_2$ line	44.6(1)

[a] Symmetry code: (i) $-x, 1-y, 1-z$. [b] Planes: for Cu1, O1, O2, N1, N12; for bpy1, N1, N12, C2−C11; for Cu$_2$O$_2$, Cu1, O1, Cu1^{i}, O1^{i}. Lines: for Cu$_2$, Cu1−Cu1^{i}. Equatorial distortion: O2−N12−N1−O1 torsion angle.

the O atoms coordinated to the Cu center being significantly longer (1.27 and 1.29 Å) than those involving the non-coordinated O atoms (1.23 Å). The copper−dihydroxymalonate six-membered chelating ring displays a boat conformation, in such a way that one hydroxyl group of the *gem*-diol functionality coordinates to the copper atom through an axial position, the Cu−OH bond length being 2.60 Å. Two structural features have their origin in the axial coordination of the hydroxyl group: on one hand, the *gem*-diol functionality shows substantially different C−OH bond lengths (1.43 and 1.38 Å for the coordinated and non-coordinated hydroxyl groups, respectively), and on the other hand, the copper coordination sphere becomes highly distorted, with an O$_{ax}$−Cu−O$_{ax}$ angle of 144°. The remaining axial position is occupied by a carboxylate O atom belonging to the centrosymmetrically related dihydroxymalonate ligand, with a Cu−O bond length of 2.49 Å. This arrangement gives rise to a dimer with an *equatorial-axial* Cu$_2$(μ^2-O)$_2$ rhomboid core, which shows O−Cu−O and Cu−O−Cu angles of 78 and 102°, respectively.

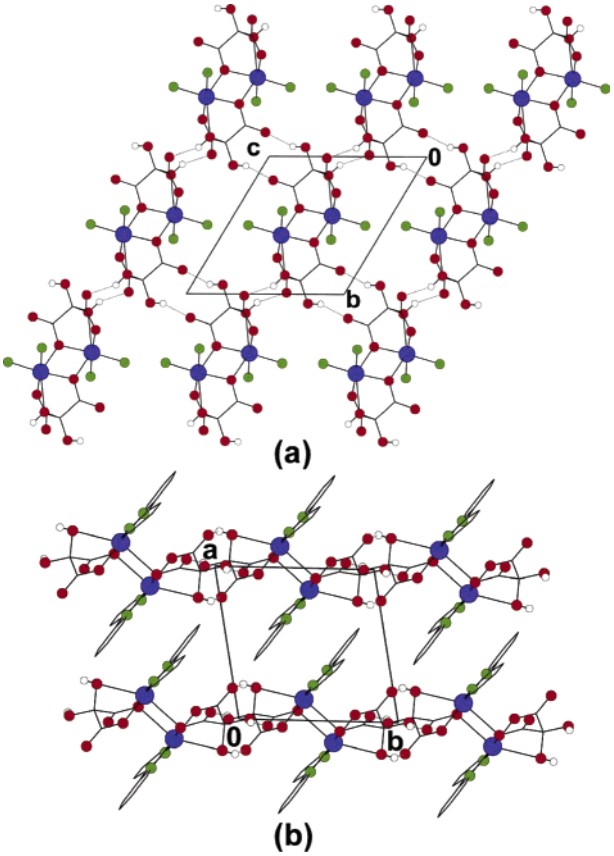

Figure 2. (a) Projection on the (100) plane of a layer of hydrogen-bonded [Cu(bpy)(dhmal)]$_2$ complexes. Bipyridine ligands have been omitted for clarity. (b) View of the crystal packing of compound **1** along the crystallographic *c* axis.

The crystal packing shows layers of dimeric complexes parallel to the *yz* plane (Figure 2a). The dimers are held together by means of an extended network of strong O−H···O hydrogen bonds involving both hydroxyl groups, and those carboxylate O atoms which are not coordinated to the copper atoms. The layers are packed along the [100] direction with the bipyridine ligands pointing to the interlamellar space (Figure 2b). They are connected through two types of weak interactions, C−H···O hydrogen bonds and π-interactions. The C−H···O hydrogen bond network involves the N1/C6 bipyridine aromatic ring, the two O atoms of the *gem*-diol functionality, and the non-coordinated O atoms of the carboxylate groups. On the other hand, the π-interactions are established between pairs of bipyridine ligands, but they lack the usual π-stacking bond-over-ring arrangement with partial overlap of the aromatic rings. This fact is due to the pronounced off-set displacement of one ligand in a direction nearly parallel to the 4-1-1′-4′ axis of the other ligand, in such a way that the C−C bridges are placed over the center of the aromatic C7/N12 rings. Table 3 summarizes the geometrical parameters of the O−H···O, C−H···O, and π-interactions.

Crystal Structure of Compound 5. To date, only one two-dimensional inorganic-metalorganic compound based on [SiW$_{12}$O$_{40}$]$^{4-}$ α-Keggin polyanions and TM-complexes can be found in the literature, namely, [{SiW$_{12}$O$_{40}$}{Cu(bpy)$_2$}$_2$]·10H$_2$O.[12i] Thus, compound **5** constitutes the second structur-

Table 3. Hydrogen-Bonding and π-Stacking Geometry in Compound **1** (Å, deg)[a]

Hydrogen Bonding				
D−H···A	D−H	H···A	D···A	D−H···A
O4−H14···O3^{i}	0.79(4)	2.00(4)	2.750(4)	158(3)
O5−H15···O6^{ii}	0.81(3)	2.11(4)	2.870(4)	157(2)
C3−H3···O4^{iii}	0.93	2.46	3.299(5)	150
C4−H4···O6^{iv}	0.93	2.54	3.447(5)	164
C5−H5···O3^{iv}	0.93	2.38	3.310(5)	173
C11−H11···O5^{i}	0.93	2.36	3.197(6)	150

π-Stacking[b]				
	DC	DZ	ANG	DXY
Cg(1)−Cg(2)^{v}	4.119(3)	3.523	10.02	2.133
Cg(1)−Cg(1)^{v}	4.078(3)	3.588	0.00	1.939

[a] Symmetry codes: (i) $-x, -y, 1-z$; (ii) $-x, -y, 2-z$; (iii) $1-x, 1-y, 1-z$; (iv) $1+x, 1+y, -1+z$; (v) $1-x, 1-y, -z$. [b] Cg(i): centroid of the aromatic ring i ($i = 1$: C7, C8, C9, C10, C11, N12; $i = 2$: N1, C2, C3, C4, C5, C6). DC: Distance between ring centroids. DZ: Perpendicular distance of Cg(i) on ring j. ANG: dihedral angle between planes i and j. DXY: Distance between the projection of Cg(i) on ring j and Cg(j).

ally characterized example of this type of hybrid compounds. It crystallizes in the monoclinic space group $P2_1/n$ with half a centrosymmetric $[SiW_{12}O_{40}]^{4-}$ Keggin polyanion, one $[Cu_2(bpy)_2(H_2O)(ox)]^{2+}$ cationic dimer and eight hydration water molecules in the asymmetric unit. Figure 3 shows the ORTEP view of a fragment of the two-dimensional hybrid network, containing one polyanion linked to four dimers, together with the atom labeling scheme.

The inorganic building block $[SiW_{12}O_{40}]^{4-}$ shows the characteristic structure of the α-Keggin isomer, which consists of a central SiO_4 tetrahedron surrounded by four vertex-sharing W_3O_{13} trimers that result from the association of three edge-sharing MO_6 octahedra, in such a way that the ideal polyanion has T_d symmetry. Since it lies on a center of inversion, the central SiO_4 tetrahedron is disordered over two crystallographic positions leading to a distorted cube. The W−O bond distances are concordant with those observed in the barium[48] or the tetramethylammonium[49] salts. They fall within the ranges 2.34−2.49 Å for central oxygen atoms coordinated to Si and W centers, 1.84−1.94 Å for bridging oxygen atoms between WO_6 octahedra, and 1.66−1.68 Å for terminal oxygen atoms.

Selected bond lengths and angles for the metal−organic building block $[Cu_2(bpy)_2(H_2O)(ox)]^{2+}$ are given in Table 4. It is made of two copper atoms bridged by an oxalate anion in the usual bis(bidentate) fashion with a Cu···Cu distance of 5.16 Å. The coordination geometries around each copper atom are significantly different, tetragonally elongated ocathedral $CuN_2O_2O'_2$ for Cu1 and square-pyramidal CuN_2O_2O' for Cu2. In both cases, the equatorial/basal planes are formed by two oxalate O atoms and two bipyridine N atoms, the Cu−O and Cu−N bond lengths ranging from 1.94 to 2.01 Å. For Cu1, the axial positions are accupied by terminal oxygen atoms of two Keggin subunits, the Cu−O_t bond lengths and Cu−O_t−W angles being almost identical (around 2.55 Å and 135.5°, respectively). In the case of Cu2, a water molecule occupies the apical position at 2.14 Å. The μ-oxalatodicopper complex displays a chair conformation, the copper equatorial/basal planes forming dihedral angles of 6 and 11° with the bipyridine and oxalato ligands, respectively. In addition to this structural distortion, the dimer is also twisted with respect to the Cu1−Cu2 axis, in such a way that the dihedral angle between the two bipyridine planes is 18°.

The crystal structure shows α-Keggin subunits placed at the center and at the vertices of the unit cell. Each polyanion is linked to the four nearest neighbors in the [111] and $[\bar{1}1\bar{1}]$ directions through four μ-oxalatodicopper complexes and, more specifically, through axial coordination of the Cu1 atoms to the terminal oxygen atoms of adjacent W1 and W4 octahedra. This type of linking between building blocks gives rise to hybrid layers parallel to the $(10\bar{1})$ plane, which are based on rhombi of 13.4 × 24.3 Å diagonals as basic structural motif (Figure 4a). The layers are packed along the c axis with the metal−organic blocks pointing to the interlamellar space. In this way, the bpy2−Cu2−ox fragments act as interlamellar separators, leading to an open-framework crystal packing with trapezoidal tunnels of 7.5 × 6 Å ($\alpha \sim 109°$) dimensions along the [010] direction (Figure 4b). These tunnels host a cascade of hydration water molecules which connect adjacent layers through an extended and intrincate network of strong O−H···O hydrogen bonds involving oxygen atoms of both inorganic and metal−organic building blocks. The hybrid layers are further connected by means of Cu···π interactions established between pairs of bpy2−Cu2−ox fragments. These fragments are arranged in such a way that the Cu2 atoms are placed over the C27/N32 aromatic rings at 3.60 Å from the ring-plane and 3.71 Å from the ring-centroid, the Cu2···Cu2 distance being 4.66 Å.

EPR Spectroscopy. Figure 5 shows the room-temperature X- and Q-band EPR powder spectra for compound **1**. At lower temperatures there is a large increase of the intensity of all the signals but their position, line shape and resolution are essentially the same. The room-temperature X-band spectrum is rather complex with four signals centered at about 2500, 2950, 3220, and 3600 G. In addition, a low-field resonance corresponding to a $\Delta M_s = \pm 2$ forbidden transition is clearly observed. At a first glance the Q-band spectrum appears to be the sum of an axial signal plus a weaker contribution. However, the extrapolation of the positions of the Q-band signals to the X-band spectrum reveals the presence of a first-order independent field phenomenon, as dipolar or pseudo-dipolar interactions. In fact, both spectra are characteristic of a triplet spin state with a small and anisotropic zero-field splitting tensor. The observation of the $\Delta M_s = \pm 2$ line indicates that the Cu(II) dimeric entities are well-isolated from the magnetic point of view. We have tried to fit the spectra using the reported formulas for the transition fields along the principal axes,[50] but no reasonable fitting was obtained, suggesting the existence of noncollinear **g** and **D** tensors. This misalignment

(48) Kobayashi, A.; Sasaki, Y. *Bull. Chem. Soc. Jpn.* **1975**, *48*, 885.
(49) Fuchs, J.; Thiele, A.; Palm, R. *Z. Naturforsch.* **1981**, *36B*, 161.
(50) Wasserman, E.; Snyder, L. C.; Yager, W. A. *J. Chem. Phys.* **1964**, *41*, 1763.

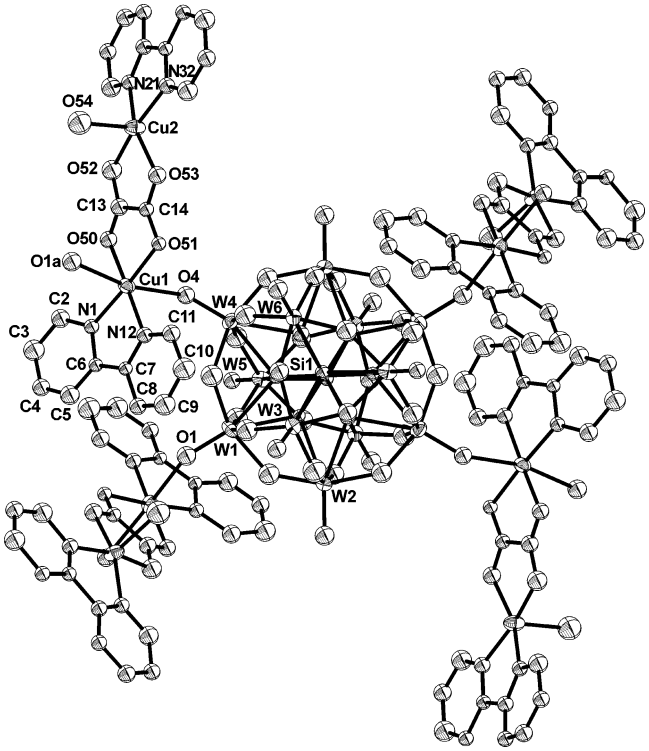

Figure 3. ORTEP view of a fragment of the two-dimensional hybrid network in compound **5**, containing one $[SiW_{12}O_{40}]^{4-}$ polyanion linked to four $[Cu_2(bpy)_2(H_2O)(ox)]^{2+}$ dimers, together with the atom labeling scheme. Hydrogen atoms have been omitted for clarity.

Table 4. Selected Bond Lengths (Å) and Angles (deg) for the Metal−Organic Block of Compound **5**[a,b]

Cu1 coordination sphere		Cu2 coordination sphere	
Cu1−O50	1.96(2)	Cu2−O52	1.96(2)
Cu1−O51	2.01(1)	Cu2−O53	1.99(2)
Cu1−N1	1.96(2)	Cu2−N21	2.00(2)
Cu1−N12	2.00(2)	Cu2−N32	1.94(2)
Cu1−O1	2.56(2)	Cu2−O54	2.14(2)
Cu1−O4^{i}	2.54(2)		
Cu1···Cu2	5.158(2)		
O50−Cu1−O51	85.4(7)	O52−Cu2−O53	84.0(8)
N1−Cu1−N12	82.3(8)	O52−Cu2−N32	168.3(8)
O1−Cu1−O4^{i}	168.5(6)	O53−Cu2−N21	161.6(7)
O1−Cu1−Cu2−O54	9.4(8)	N21−Cu2−N32	80.8(8)
Cu1−bpy1	5.4(8)	Cu2−bpy2	6.0(8)
Cu1−ox	11.1(8)	Cu2−ox	10.6(8)
bpy1−ox	14.9(8)	bpy2−ox	16.3(8)
equatorial distortion	4.6(8)	equatorial distortion	5.5(8)
	Cu1−Cu2	8.2(8)	
	bpy1−bpy2	17.8(8)	

[a] Symmetry code: (i) $^1/_2 - x$, $^1/_2 - y$, $^1/_2 - z$. [b] Planes: for Cu1, O50, O51, N1, N12; for Cu2, O52, O53, N21, N32; for ox, O50, O51, C13, C14, O52, O53; for bpy1, N1, N12, C2−C11; for bpy2, N21, N32, C22−C31. Equatorial distortion: N1−N12−O51−O50 (Cu1) and N21−N32−O53−O52 (Cu2) torsion angles.

between **g** and **D** is not surprising taking into account the fact that the copper−copper intradimer direction deviates strongly from the normal to the equatorial planes of the Cu(II) cromophores.[51]

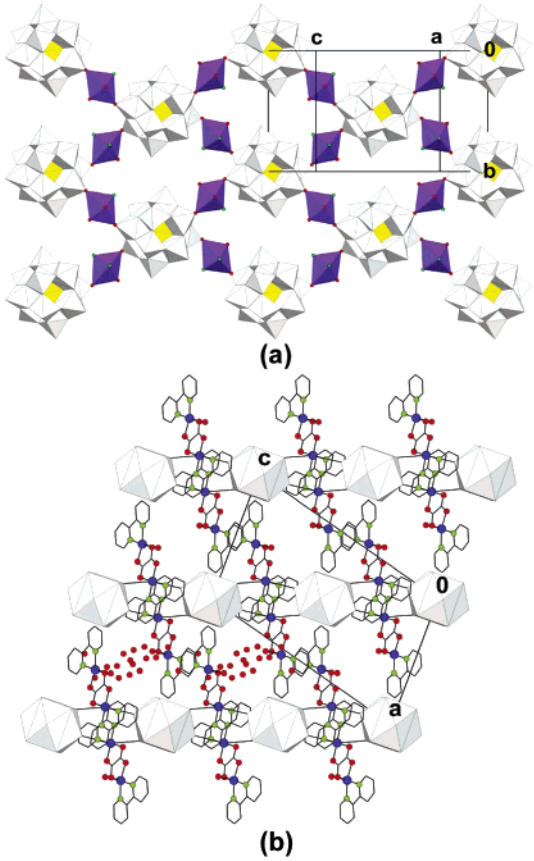

Figure 4. (a) Polyhedral projection of a hybrid layer of compound **5** on the (10$\bar{1}$) plane. Cu2 atoms, oxalato bridges, and bipyridine ligands have been intentionally supressed to clearly illustrate the linkage of the Keggin polyanions through the coordination sphere of the Cu1 atoms. (b) View of the crystal packing of compound **5** along the crystallographic *b* axis. Keggin polyanions are represented as cubooctahedra for clarity.

Figure 6 shows the room- and low-temperature X- and Q-band EPR powder spectra for compound **5**. At room temperature, it gives rise to a single anisotropic broad resonance centered at ca. 3250 G in the X-band spectrum and at ca. 11 700 G in the Q-band one. These resonances can be simulated as a rhombic signal with the best fit parameters $g_1 = 2.218$, $g_2 = 2.120$, and $g_3 = 2.057$ ($\langle g \rangle = 2.132$) and $g_1 = 2.245$, $g_2 = 2.130$, and $g_3 = 2.060$ ($\langle g \rangle = 2.145$) for the X- and Q-band experiments, respectively. The absence of transitions associated with a well-isolated triplet spin state clearly indicates that a nonnegligible magnetic interaction must take place between the copper−oxalate dimers, so that the rhombic signal can be attributed to an exchange **g** tensor. According to our previous studies in analogous one-dimensional systems,[52] Keggin polyanions are effective in transmitting intermolecular magnetic interactions between copper−oxalate dimers that are supported on the terminal oxygen atoms of adjacent WO_6 octahedra. Therefore, an exchange pathway between the Cu1 atoms through the $[SiW_{12}O_{40}]^{4-}$ subunits can be proposed, although the participation in the magnetic exchange of the Cu···π interactions involving the Cu2 atoms cannot be a priori disregarded (Figure S6 of the Supporting Information). The intensity of the signal diminishes as the temperature is lowered, in line

(51) Bencini, A.; Gatteschi, D. *Electron Paramagnetic Resonance of Exchange Coupled Systems*; Springer-Verlag: Berlin, Germany, 1990.

(52) Reinoso, S. Ph.D. thesis, Universidad del País Vasco, Spain, 2005.

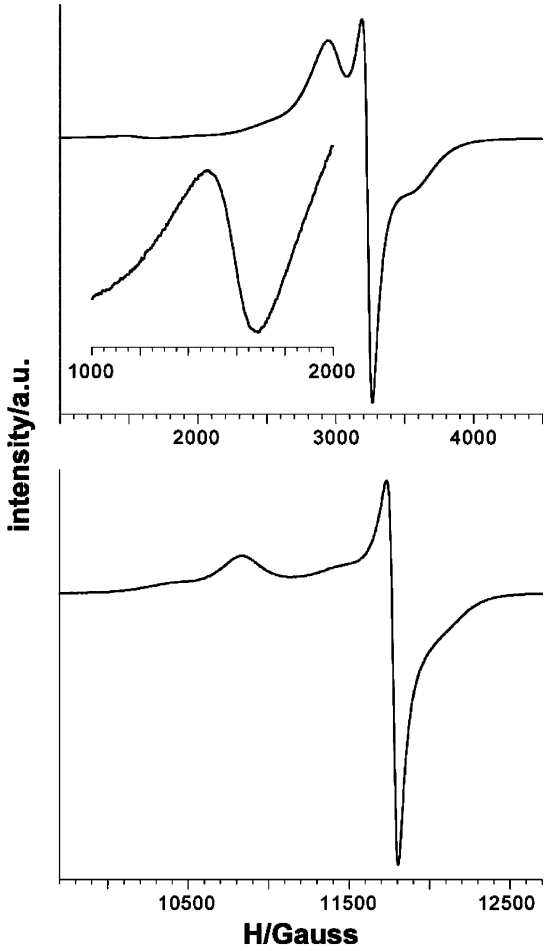

Figure 5. Room-temperature X-band (top) and Q-band (bottom) EPR powder spectra of compound **1**.

with the strong intramolecular antiferromagnetic coupling expected for the copper−oxalate dimer considering its coplanar orbital topology. This fact allows the observation of a magnetically isolated monomeric impurity in the low-temperature X-band spectrum. Its contribution shows a poorly resolved hyperfine structure on the parallel region (ca. 2800 G), and it can be simulated by using an axial **g** tensor with the values of its principal components analogous to those reported for the $[SiW_{11}O_{39}Cu(H_2O)]^{6-}$ polyanion.[15,53] This fact indicates that, when the $[SiW_{11}O_{39}Cu(H_2O)]^{6-}$ Keggin-type polyanion is used as the POM precursor, it is not possible to completely separate compound **5** from the potassium salt of the $[\{SiW_{11}O_{39}Cu(H_2O)\}\{Cu_2(bpy)_2(H_2O)_2(ox)\}_2]^{2-}$ hybrid polyanion (compound **4**) by using fractional crystallization techniques.

Magnetic Properties. Figure 7 shows the thermal evolution of the magnetic molar susceptibility and the $\chi_m T$ product ($\chi_m T = \mu_{eff}^2/8$) for compounds **1** and **5**. For compound **1**, the magnetic susceptibility experiments a continuous increase with decreasing temperature and the χ_m vs T curve shows no remarkable feature. Above 30 K, the data are well-described by a Curie−Weiss law with a Curie constant of

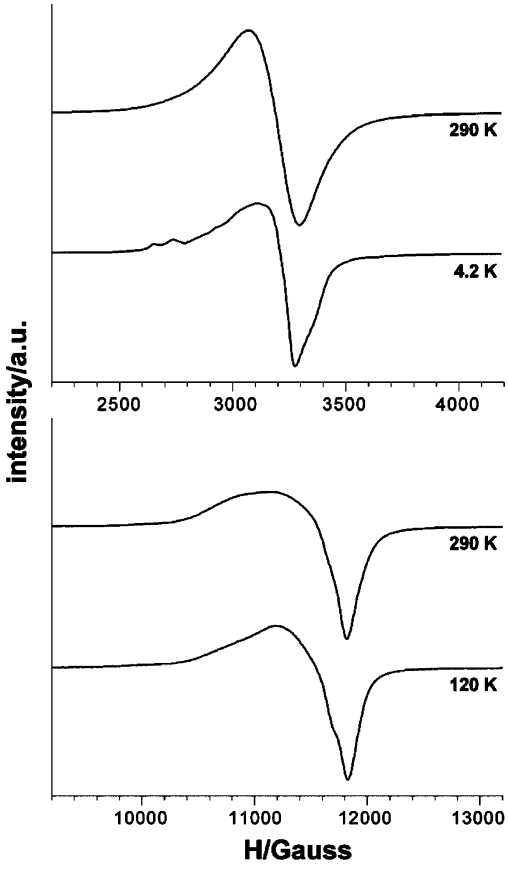

Figure 6. High- and low-temperature X-band (top) and Q-band (bottom) EPR powder spectra of compound **5**.

0.85 $cm^3 \cdot K \cdot mol^{-1}$ and a Weiss temperature of +1.2 K. This positive temperature intercept suggests the predominance of ferromagnetic interactions in this compound, and it is consistent with the overall appearance of the $\chi_m T$ vs T curve. At room temperature, the $\chi_m T$ product is equal to 0.85 $cm^3 \cdot K \cdot mol^{-1}$, which is the expected value for two uncoupled Cu(II) ions with a g value of 2.13. It slightly increases upon cooling below 30 K and reaches a value of 1.10 $cm^3 \cdot K \cdot mol^{-1}$ at 2 K. The rise in magnetic moment is small but unambiguous, and it is indicative of ferromagnetic couplings. To confirm the ferromagnetic nature of the dominant interactions, magnetization versus field measurements have been carried out at our lowest available temperature (2 K). Under a magnetic field of 70 kG, the magnetization is practically saturated with a maximum value of $M(N\beta)^{-1} = 2.09$, which corresponds to the theoretical saturation value for two unpaired electrons with an average g value of 2.12. The resulting curve (included as Supporting Information) has been compared with the Brillouin function showing a more rapid saturation than that expected for a strictly paramagnetic system.[54] Therefore the ferromagnetic coupling is predominant in compound **1**. As expected for a system without appreciable long-range interactions, no remanent magnetization neither coercitive fields have been observed. The observed behavior is in good agreement with the parallel orbital topology of the dimer. The two singly occupied

(53) (a) Scholz, G.; Lück, R.; Stöβer, R.; Lunk, H.-J.; Ritschl, F. *J. Chem. Soc., Faraday Trans.* **1991**, *87*, 717. (b) Gamelas, J. A.; Santos, I. C. M. S.; Freire, C.; de Castro, B.; Cavaleiro, A. M. V. *Polyhedron* **1999**, *18*, 1163.

(54) Carlin, R. L. *Magnetochemistry*; Springer-Verlag: Berlin, Germany, 1986.

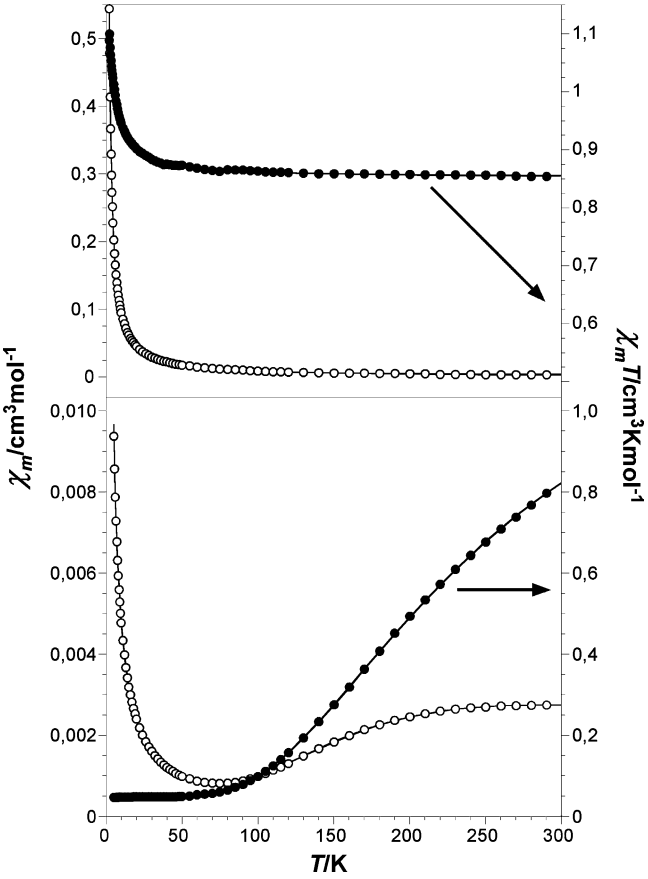

Figure 7. Thermal evolution of the magnetic susceptibility and the $\chi_m T$ product for compounds **1** (top) and **5** (bottom). Continuous lines represent the least-squares fit to eq 1.

molecular orbitals (SOMOs) of the Cu(II) ions ($d_{x^2-y^2}$) are parallel between them and perpendicular to the exchange pathway through the dihydroxymalonate bridge, as can be clearly seen in the DFT calculated magnetic orbitals, obtained as a linear combination of the SOMOs (Figure 8). In this situation, the overlap between both magnetic orbitals are close to zero and only weak couplings, ferro- or antiferromagnetic, can be expected.

In the case of compound **5**, the room temperature χ_m value is 2.78×10^{-3} cm^3·mol^{-1} and it rapidly decreases with decreasing temperature, in such a way that neither a maximum nor a Curie−Weiss behavior is observed. The χ_m curve reaches a minimum at around 70 K (0.82×10^{-3} cm^3·mol^{-1}) from which it strongly increases to a value of 9.37×10^{-3} cm^3·mol^{-1} at 5 K. On the other hand, the room-temperature $\chi_m T$ value (0.83 cm^3·K·mol^{-1}) is substantially lower than that expected for four Cu^{II} ions per formula unit, considering them to be uncoupled ions with $g = 2$ (1.50 cm^3·K·mol^{-1}). When the system is cooled down, the $\chi_m T$ product rapidly decreases from 300 to ca. 70 K and it remains approximately constant below this temperature, reaching a value of 0.05 cm^3·K·mol^{-1} at 5 K. This behavior indicates the presence of very strong antiferromagnetic interactions, together with the contribution of a small fraction of paramagnetic impurities, so that the local maximum in the χ_m curve is expected to be masked. This observation is in agreement with the structural features of the copper−oxalate

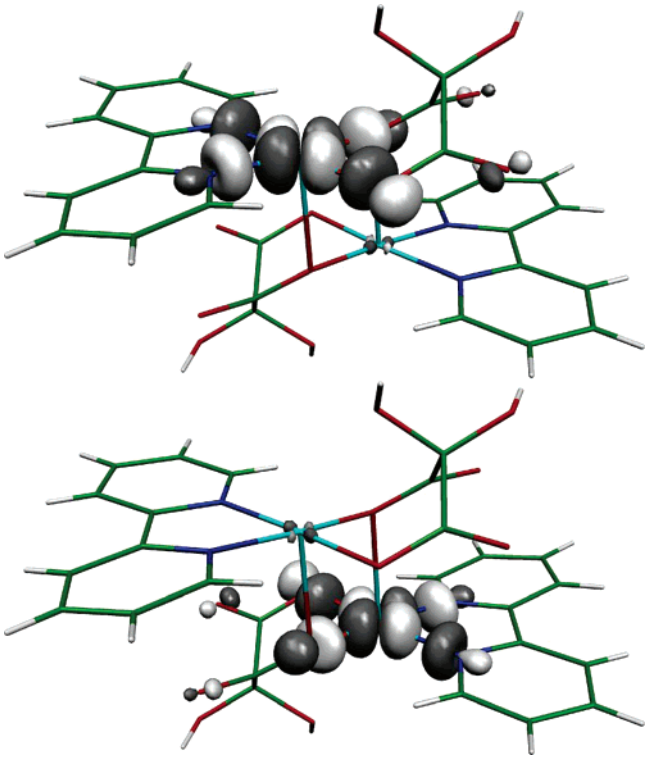

Figure 8. Singly occupied molecular orbitals (SOMOs) of compound **1**, calculated with the B3LYP functional and a triple-ζ valence basis set in all atoms.

dimer in compound **5**, which shows Cu^{II}-equatorial planes almost coplanar with the oxalato ligand (coplanar orbital topology). In this situation, the Cu^{II}-equatorial $d_{x^2-y^2}$ magnetic orbital is directed toward the oxalate frontier orbitals, so that the antiferromagnetic contribution is maximized and exchange coupling constants ranging from −300 to −400 cm^{-1} are usually observed.

The experimental curves of compounds **1** and **5** have been compared with those calculated with the following general expression

$$\chi_m = (1-\rho)\frac{ANg^2\beta^2}{kT[3+\exp(-J/kT)]} + \rho\frac{N(g')^2\beta^2}{4kT} \qquad (1)$$

where N, β, and k have their usual meanings and g is the average g-factor of the copper−oxalate or copper−dihydroxymalonate dimers. The first term in the above expression is the classical Bleaney−Bowers[55] equation for a dinuclear Cu^{II} complex, expressed per copper atom and modified to take into account the presence of noncoupled impurities. The singlet−triplet energy gap (J) is defined by the Hamiltonian $H = -JS_AS_B$ ($S_A = S_B = {}^1/_2$), whereas the A factor represent the number of Cu^{II} ions per formula unit ($A = 2$ and $A = 4$ for compounds **1** and **5**, respectively). The second term corresponds to the paramagnetic contribution of the noncoupled impurities, ρ being their fraction and g' being their local g-factor. According to the EPR spectra, compound **1** is almost free of impurities, and therefore ρ was fixed to zero during the fitting process. In the case of compound **5**,

(55) Bleaney, B.; Bowers, K. D. *Proc. R. Soc. London, Ser. A* **1952**, *214*, 451.

EPR spectroscopy shows that the noncoupled impurities mainly consist of copper−monosubstituted $[SiW_{11}O_{39}Cu(H_2O)]^{6-}$ Keggin polyanions, so that g' was fixed to the value reported in the literature (2.205).[15] Although the EPR spectra also indicate that the copper−oxalate dimers in compound **5** are magnetically coupled, the magnitude of the interdimeric coupling through the Keggin polyanions is expected to be negligible in comparison with the intradimeric one, and therefore interdimeric interactions have been intentionally suppressed from eq 1 to avoid an excessive number of variables.

Least-squares fits of eq 1 to the experimental data were performed by minimizing the following function

$$R = \{\sum_{i=1}^{NP}[\chi_m(exp)_i - \chi_m(cal)_i]^2/(NP - NV)\}^{1/2} \qquad (2)$$

where NP is the number of data points and NV is the number of variable parameters. The best fit results are $J = +3.4$ cm^{-1}, $g = 2.13$, and $R = 1.1 \times 10^{-3}$ for compound **1** and $J = -331$ cm^{-1}, $g = 2.134$, $\rho = 10.6\%$, and $R = 3.8 \times 10^{-4}$ for compound **5**.

The exchange coupling constant of compound **1** is in very good agreement with the DFT calculated ones, which are weakly ferromagnetic and in the range $+3.2$ to $+3.5$ cm^{-1}, depending on the size of basis set used, and is $+3.4$ cm^{-1} with the best quality basis set: QZVPP on the copper atoms and TZVPP on the rest.

In the case of compound **5**, the observed exchange coupling constant is in good agreement with those observed for several compounds containing $[\{Cu(bpy)\}_2(\mu\text{-ox})]^{2+}$ complexes of coplanar orbital topoly,[34,56] which range from -330 to -390 cm^{-1}. However, the J value is 20 cm^{-1} less antiferromagnetic than those calculated for analogous one-dimensional systems based on Keggin-type polyanions and centrosymmetric copper−bypiridine−oxalate dimers with an almost planar conformation.[15b] This weakening of the antiferromagnetic coupling in compound **5** with respect to the one-dimensional systems can be attributed to two different types of structural factors. On one hand, the copper−oxalate dimer is composed of two copper atoms with different coordination geometries (octahedral and square-pyramidal), a fact that weakens the magnetic coupling according to Kahn's equation.[57] On the other hand, the dimer shows a chairlike conformation and it is twisted with respect to the Cu−Cu axis (with an angle of 8° between the equatorial/basal planes), both structural distortions decreasing the overlapping of the magnetic orbitals with the frontier orbitals of the oxalato bridge, as shown by computational calculations.[58]

(56) (a) Julve, M.; Faus, J.; Verdaguer, M.; Gleizes, A. *J. Am. Chem. Soc.* **1984**, *106*, 8306. (b) Gleizes, A.; Julve, M.; Verdaguer, M.; Real, J. A.; Faus, J.; Solans, X. *J. Chem. Soc., Dalton Trans.* **1992**, 3209. (c) Castillo, O.; Muga, I.; Luque, A.; Gutiérrez-Zorrilla, J. M.; Sertucha, J.; Vitoria, P.; Román, P. *Polyhedron* **1999**, *18*, 1235.

(57) Kahn, O. *Molecular Magnetism*; VCH: New York, 1993.

(58) (a) Cano, J.; Alemany, P.; Alvarez, S.; Verdaguer, M.; Ruiz, E. *Chem. Eur. J.* **1998**, *4*, 476. (b) Alvarez, S.; Julve, M.; Verdaguer, M. *Inorg. Chem.* **1990**, *29*, 4500.

Conclusions

In the presence of Cu^{II} and 2,2′-bipyridine in an aqueous acidic medium, tetrahydroxy-*p*-benzoquinone oxidizes to give croconate, which undergoes further ring-opening oxidation to decompose into dihydroxymalonate and oxalate dianions. On the basis of the literature, a possible mechanism for the oxidation of the benzoquinone into croconate is proposed. We have made use of this "slow source" behavior to isolate under open-air mild reaction conditions the neutral dimer $[Cu(bpy)(dhmal)]_2$ (**1**) and the inorganic−metalorganic hybrid compound $[\{SiW_{12}O_{40}\}\{Cu_2(bpy)_2(H_2O)(ox)\}_2]\cdot 16H_2O$ (**5**) as single crystals suitable for X-ray diffraction. Compound **1** constitutes the first structurally characterized example of a transition metal−dihydroxymalonate complex, and it contains two copper atoms bridged by two dihydroxymalonato ligands acting in a μ^2-κ^3O,O′,O″:κ^1O coordination fashion, so that an equatorial−axial $Cu_2(\mu^2\text{-}O)_2$ rhomboid core is formed. On the other hand, compound **5** shows a two-dimensional arrangement of Keggin polyanions linked by one of the Cu atoms of the oxalate cationic dimers to give hybrid layers parallel to the $(10\bar{1})$ plane, the remaining oxalato−Cu−bipyridine fragments acting as interlamellar separators. EPR and magnetic susceptibility studies shows a relatively weak ferromagnetic coupling for the $Cu_2(\mu^2\text{-}O)_2$ rhomboid core of compound **1** and a strong intradimeric antiferromagnetic coupling, together with interdimeric magnetic interactions, in the case of the copper−oxalate dimers of compound **5**. DFT calculations have offered invaluable help since they have been successfully applied, on one hand to confirm the ferromagnetism in compound **1** and on the other hand to obtain a complete band assignment of the experimental FT-IR spectra of both compounds.

Acknowledgment. This work was supported by Universidad del País Vasco (Grant 9/UPV 00169.310-15329/2003) and Ministerio de Ciencia y Tecnología (Grant MAT2005-03047). S.R. thanks Gobierno Vasco for his Doctoral Fellowship. The SGI/IZO-SGIker UPV/EHU (supported by the National Program for the Promotion of Human Resources within the National Plan of Scientific Research, Development and Innovation-Fondo Social Europeo and MCyT) is gratefully acknowledged for generous allocation of computational resources.

Supporting Information Available: Magnetization vs field measurements of compound **1** and comparison with the Brillouin function, thermogravimetric curves of compounds **1** and **5**, powder X-ray diffractograms of compounds **1**, **3**, and **5**, possible exchange pathways between $[Cu_2(bpy)_2(H_2O)(ox)]^{2+}$ dimers proposed for compound **5**, and X-ray crystallographic files of compounds **1** and **5** in CIF format. This material is available free of charge via the Internet at http://pubs.acs.org.

IC061671M